



ELSEVIER

Available online at www.sciencedirect.com

ScienceDirect

journal homepage: www.elsevier.com/locate/he

Synergistic enhancement of biohydrogen production by supplementing with green synthesized magnetic iron nanoparticles using thermophilic mixed bacteria culture

Ainul Husna Abdul Aziz ^{a,*}, Nurul Sakinah Engliman ^{a,**},
 Mariatul Fadzillah Mansor ^a, Peer Mohamed Abdul ^b,
 Shalini Narayanan Arisht ^b, Nur Syakina Jamali ^c, Ming Foong Tiang ^b

^a Department of Chemical Engineering and Sustainability, Kulliyah of Engineering, International Islamic University Malaysia (IIUM), P.O. Box 10, 50728, Gombak, Kuala Lumpur, Malaysia

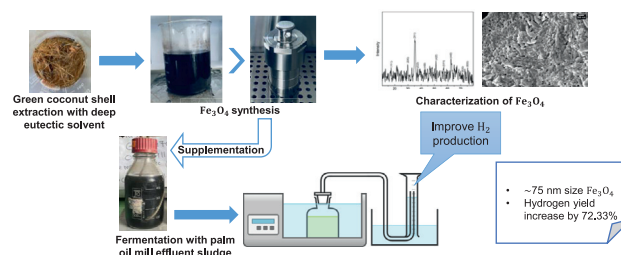
^b Research Centre for Sustainable Process Technology (CESPRO), Faculty of Engineering and Built Environment, Universiti Kebangsaan Malaysia (UKM), 43600, Bangi, Selangor, Malaysia

^c Department of Chemical and Environmental Engineering, Faculty of Engineering, Universiti Putra Malaysia, Serdang 43400, Malaysia

HIGHLIGHTS

- Green synthesis of super-paramagnetic iron nanoparticles (NPs) at ~75 nm size was produced using plant extract.
- Magnetic iron NPs at 200 mg Fe/L improved biohydrogen yield by 72.33%, enhanced sugar utilization, and shorten the lag phase.
- Kinetics study using Gompertz and Monod model showed that added iron NPs have improved the kinetic parameters than control.

GRAPHICAL ABSTRACT



ARTICLE INFO

Article history:

Received 31 May 2022

Received in revised form

30 August 2022

Accepted 11 September 2022

Available online xxx

ABSTRACT

The production of biohydrogen can be improved by focusing on the nutrients needed by fermentative bacteria like iron. Iron reacts with the [Fe-Fe]-hydrogenase enzyme within the mixed bacteria culture for optimum hydrogen release. Iron nanoparticles (NPs) are attractive due to its unique properties and high reactivity. It can be produced through green synthesis, a more eco-friendly and relatively lower cost process, by using iron salt as precursor and green coconut shell extracted by deep eutectic solvent (DES) as reducing

Abbreviations: Nanoparticles, NPs.

* Corresponding author.

** Corresponding author.

E-mail addresses: ainulhusnaabdulaziz@gmail.com (A.H. Abdul Aziz), sakinahengliman@iium.edu.my (N.S. Engliman).

<https://doi.org/10.1016/j.ijhydene.2022.09.105>

0360-3199/© 2022 Hydrogen Energy Publications LLC. Published by Elsevier Ltd. All rights reserved.

Keywords:

Biohydrogen production
Mixed bacteria culture
Green synthesized magnetic nanoparticles

agent. The coconut shell extract consists of phytochemicals that help in producing poly-disperse magnetic iron oxide nanoparticles at ~75 nm in size. The addition of optimum concentration of 200 mg Fe/L magnetic iron NPs resulted in the maximum cumulative hydrogen production, glucose utilization and hydrogen yield of 101.33 mL, 9.12 g/L and 0.79 mol H₂/mol glucose respectively. Furthermore, the kinetic analysis on Gompertz model using the optimum magnetic iron NPs concentration showed that the hydrogen production potential (P) and hydrogen production rate (R_m) increased to 50.69 mL and 3.30 mL/h respectively and the lag phase time reduced about 7.12 h as compared with the control experiment (0 mg Fe/L). These results indicated the positive effects of magnetic iron NPs supplementation on fermentative biohydrogen production of mixed bacteria culture and proved the feasibility of adding the magnetic iron NPs as the micronutrient for enhancement of such hydrogen production system.

© 2022 Hydrogen Energy Publications LLC. Published by Elsevier Ltd. All rights reserved.

Statement of novelty

- The novelty of this research can be highlighted in the application of green synthesis of magnetic iron nanoparticles using green coconut shell extracted using deep eutectic solvent. Later the synthesized magnetic iron nanoparticles was proven to improve the biohydrogen fermentation with mixed thermophilic bacteria as well as enhanced the sugar utilization and shorten the lag phase.
- The operating condition particularly temperature used in this study was higher than those reported in other studies related to application of metal nanoparticles, it would be inferred that the coupling effect of higher temperature and the presence of magnetic iron nanoparticles promoted the improvement in biohydrogen production as well as enhancing the substrate consumption and hydrogen yield.

Introduction

Biohydrogen opens potential to replace the depleting fossil fuel use in the future. This renewable energy is attractive as it does not produce toxic by-products and only produces water after combustion. This clean energy source consists of energy density up to 142 kJ/g [1]. Dark fermentation with thermophilic bacteria is an efficient way to produce biohydrogen and it has been used by many as it is considered as low cost process, versatile and sustainable [2]. In fermentation for biohydrogen production, the use of carbohydrates as the carbon source is highly preferred due to its ability to produce higher amounts of acetic and butyric acids together with hydrogen gas [3]. The metabolic pathway applied when using obligate anaerobes is the pyruvate ferredoxin oxidoreductase pathway, where the glucose breaks down into pyruvate followed by acetyl-CoA. From this point, the acetyl-CoA can change into ethanol, acetate, or butyryl-CoA that will turn into butyrate [3]. During this pathway, the hydrogenase enzyme facilitates the production of hydrogen, specifically during the pyruvate to acetyl-CoA conversion.

There are three types of hydrogenases; [Ni-Fe]-hydrogenase, [Fe-Fe]-hydrogenase, and [Fe]-hydrogenase

where each are activated under different situations. Both the [Ni-Fe]-hydrogenase and [Fe-Fe]-hydrogenase are activated under fermentation and energy conservation whereas the [Fe]-hydrogenase is activated under fermentation only. Under the mechanism of dark fermentation, [Fe-Fe]-hydrogenase is optimum in biohydrogen production since [Ni-Fe]-hydrogenase is less efficient due to the requirement of higher amount of energy (ATP) input to catalyse the process and the [Fe]-hydrogenase does not catalyse the biohydrogen reversible redox reaction [4].

To improve the bacterial growth and in turn the hydrogen production, metal oxides such as iron, nickel, copper and zinc have been researched as trace elements that act as micronutrient to the bacteria [5–8]. These studies used nano-size trace metal due to its unique characteristics of being very small in size, very high in surface area and having high reactivity. Out of all these metal nanoparticles, iron specifically does not only act as micronutrient to the bacteria, but it is also essential in the formation of ferredoxin and hydrogenase under the pyruvate ferredoxin oxidoreductase pathway. It is also used as co-factor to [Fe-Fe]-hydrogenase that is active under dark fermentation conditions [9]. Studies using iron nanoparticles showed high increase of hydrogen yield under dark fermentation [5,10–12]. The use of conductive magnetic iron nanoparticles has proved to facilitate the microbial electron transfer which is the essence in better performance of hydrogen production [1]. The addition of magnetite (Fe₃O₄) helps in forming the electronic conductor chains that improves the efficiency of electronic transport in the mixed bacteria culture and enhances the co-enzymes activity. The Fe₃O₄ corrosion produces Fe²⁺ as a by-product which then heightens the soluble microbial products content effectively that also helps in ethanol-producing bacteria growth [13]. Furthermore, nanoparticles are normally used in trapping and storing electrons which enables further reduction of protons H⁺ to H₂, helping in the production of hydrogen in this case [14]. In some study made by using magnetite in methanogen production, the researchers found that magnetite aggregates with microbes and can be separated and recycled for future use which also helped in retaining more biomass in the process [15].

Magnetic iron nanoparticles can be bought commercially or synthesized through physical, chemical, or biological

method. However, many conventional syntheses are harmful to environment, uses toxic chemicals and pose many disadvantages such as requires high temperature and critical pressure in order to control its size [16]. Thus, a greener alternative is needed to produce magnetic iron nanoparticles. The use of plant extract from biomass waste is one of the biological methods that can be implemented. The biomass waste can be utilized by extracting the phytochemicals which act as the reducing agent to the iron salt precursor.

Therefore, coconut shells were used in this study due to the abundance in Malaysia. Local street vendors throw away the shells once coconut juice is extracted and put away into landfills whereas the chemical compounds in the shells can be utilized for nanoparticle synthesis. The coconut shells extract was collected through extraction method using deep eutectic solvent (DES) method as it is the greener way to extract the active compound from plant compared to ionic liquid. DES are eutectic mixtures of two or more chemicals that have hydrogen donor and hydrogen acceptor properties. The low lattice energy of the mixture makes it have lower melting point than the individual chemical separately [17]. The properties of DES such as low viscosity and high density, aids in separation of phases in the matrix during extraction [18]. The plant extract mediated nanoparticles were used to investigate the effect of supplementation of magnetic iron nanoparticles in term of volume of hydrogen produce, yield of hydrogen, substrate utilization as well as biomass concentration under various concentration from 0 mg Fe/L to 300 mg Fe/L. Moreover, the kinetic analysis on the hydrogen production as well as substrate consumption was determined using Gompertz and Monod equation in order to find out the enhancement of the hydrogen production.

Materials and methods

Green synthesis of magnetic iron nanoparticles

Green coconut shells were obtained from local hawker stalls while choline chloride and ascorbic acid were purchased from BT Science Sdn. Bhd. The coconut shell was cut into pieces, washed, and dried overnight at 60 °C. The deep eutectic solvent combination used was choline chloride and ascorbic acid at 2:1 M ratio in 100 mL total volume, mixed in 65 °C at 100 rpm for 30 min. The extraction process was similar to previous study with some modification [19], where 5 g of dried coconut shell pieces was extracted by 100 mL DES in room temperature at 100 rpm for 20 min. The light orange colour of DES was changed to light brown colour after extraction with coconut shell. The total phenolic compound was measured by using the Folin-Ciocalteu method followed by compound identification through gas chromatography mass spectrometry (GC-MS) with similar conditions as previous study [19]. The coconut shell extract was then used as reducing agent in green synthesis of iron nanoparticles modified from Maheswari and Reddy [20]. 60.12 mL of distilled water was poured into a 250 mL beaker. Drops of sodium hydroxide was added until the solution reached pH 10. The mixture was placed onto magnetic stirrer, set to 80 °C and 300 rpm. While heating up, 0.252 g of iron (II) chloride was added, making the mixture turn to

green followed by addition of 0.396 g of iron (III) chloride which turned the mixture into a rust brown colour. After the iron precursors were fully dissolved, 3.24 mL of the coconut extract was added dropwise. After reaching 80 °C, the mixture was left to agitate for 10 min. The mixture changed into light yellow colour before 24.12 mL of 5 M sodium hydroxide was added dropwise and left to agitate for 10 min. The mixture colour changed to black and was poured into a 100 mL hydrothermal synthesis reactor that was placed in an oil bath that was preheated to 130 °C and left for 150 min. After cooling down to room temperature, the sediments were washed with ethanol and ultra-purified water at 5000 rpm and 5 min centrifugation. Pallet collected was left to freeze dry for three days. The end product of nanoparticles synthesized was black powder.

The nanoparticles were stacked into circle placeholder for analysis using the X-ray diffractometer (XRD) equipment. The instrument used a Cu K α radiation at 45 kV with monochromatic filter at 20–80° range. Field-emission scanning electron microscope (FESEM) was used at 30,000 \times magnification to analyze the shape, size, and morphology of the nanoparticles. The zeta potential was measured using zeta potential analyzer with maintained temperature at 25 °C and each run was made 100 runs at least three times for accuracy. The magnetic property was analyzed using a vibrating sample magnetometer (VSM) at room temperature.

Mixed culture and fermentation medium

The mixed bacteria culture used in this research were obtained from palm oil mill effluent sludge of an anaerobic digester. The sludge was preheated to 80 °C for 60 min in flask with a magnetic stirrer to inactivate the methanogens. The fermentation medium used contained glucose 10 g/L; peptone 3 g/L; yeast extract 3 g/L; sodium chloride 1 g/L; sodium acetate 1 g/L; L-cysteine hydrochloride 0.5 g/L and the pH of the fermentation medium was adjusted to pH 5.5 [5].

Experimental procedures

The fabricated magnetic iron nanoparticles were applied onto the mixed bacteria culture. Using 150 mL serum bottle, 10% of mixed bacteria culture was added followed by fermentation medium until 100 mL total volume. Magnetic iron nanoparticles were added at different concentrations of 0, 25, 50, 100, 150, 200 and 300 mg Fe/L. The initial pH was adjusted to 5.5 and sparged with nitrogen gas before placed into 55 °C water bath. The accumulated biogas produced were measured using syringe and needle every day for 72 h. The final pH and optical density were recorded. The volatile fatty acids present in the culture with different concentrations of magnetic iron nanoparticles were analyzed using HPLC (Agilent 1100, California, USA with UV detector) alongside ROA column and 0.0025 M H₂SO₄ as mobile phase running at flow rate of 0.5 mL/min at 40 °C for 35 min [5]. The iron oxide concentration with highest biogas production was used for the next step. The best concentration of magnetic iron nanoparticles was used to compare with control for validation and kinetic modelling.

For kinetic experiment, the experiment was conducted using the total volume of 250 mL with 10% of mixed bacteria

culture as inoculum. The initial pH was adjusted to 5.5 and placed into 55 °C water bath. The optical density and biogas produced were measured at specific times to observe the bacterial growth curve of the bacterial culture.

Theory/calculation

Energy analysis

Hydrogen energy production rate, EPR (kJH₂/Ld) was calculated following previous study [21,22].

$$EPR = HPR/22.4 HV_{H_2} \quad (\text{Equation 1})$$

where HPR is the hydrogen production rate (LH₂/L·d) and HV_{H₂} is the heating value of hydrogen (286 J/mmol) [21,23].

Monod kinetic model

The modelling of biohydrogen production in this study was based on two kinetic models which are the Monod and the Gompertz model. The Monod kinetics equation was used to describe the substrate dependent of growth kinetic model with the aid of single substrate concentration in this equation. The equation is based on relationship between the substrate concentration and cell growth rate. The Monod equation is expressed as:

$$\mu = \frac{\mu_{max}S}{K_s + S} \quad (\text{Equation 2})$$

where K_s is the Monod cell growth saturation coefficient (g/L); μ_{max} is the maximum specific growth rate (h⁻¹). The value of K_s is similar to the substrate concentration S (g/L) when μ = 0.5 μ_{max}. The model is linearized to calculate the constant values. The linearize model is as follows:

$$\frac{1}{\mu} = \frac{K_s}{\mu_{max}} \left(\frac{1}{S} \right) + \frac{1}{\mu_{max}} \quad (\text{Equation 3})$$

where $\frac{1}{\mu}$ is the y axis, $\frac{1}{S}$ is the x axis, $\frac{K_s}{\mu_{max}}$ is the slope and the $\frac{1}{\mu_{max}}$ is the intercept point.

Gompertz model

The Gompertz function is based on an exponential relationship between specific growth rate and population density. The equation is expressed as follows:

$$N_{(t)} = C \exp\{\exp[-B(t - M)]\} \quad (\text{Equation 4})$$

where t = time, N_(t) = population density at time t, C = upper asymptotic value (maximum population density), M = time at which the absolute growth rate is maximal, and B = relative growth rate at M time.

The equation was modified to suit description of biogas production and time to see the relation between the two variables. The modified equation is as follows;

$$H = P_{max} \exp \left[- \exp \left(\frac{R_m \cdot e}{P_{max}} (\lambda - t) + 1 \right) \right] \quad (\text{Equation 5})$$

where H is the cumulative hydrogen production, P_{max} represents maximum biogas production (mL), R_m is maximum biogas production rate (mL/h), e is Euler's number at 2.73 while λ is the lag phase time (hr) and t is the incubation time (hr).

Results and discussion

Characteristic of green synthesized magnetic iron nanoparticles

The combination of choline chloride and ascorbic acid as DES extraction solvent was able to extract 3715 mg GAE/L of total phenol from green coconut shell. The use of deep eutectic solvent helped to optimize hydrogen bonding for maximum phenolic extraction compared to conventional extraction method using water [19]. Ascorbic acid in this solvent affects the extraction positively as the process utilizing the hydrogen bond between choline chloride and ascorbic acid and it helped to improve the extraction of phenolic compounds from coconut shell [24].

GC-MS analysis found that the bioactive compounds within the coconut shell extracted by DES combination of choline chloride and ascorbic acid at 2:1 M ratio were mostly antioxidants such as carotenoid, lycopene, astaxanthin, lycopene, and α-Carotene, similarly explained in previous study between water extracted coconut shell and DES extracted coconut shell [19]. There were four phenolic compounds present within the extract, which were 1,2,4-Benzenetricarboxylic acid, 1,2-dimethyl ester, the 2-Nonaprenyl-6-methoxyphenol, the Trimethyl[4-(1,1,3,3,-tetramethylbutyl)phenoxy]silane, and the 2',6'-Bis(trimethylsiloxy)-acetophenone. These compounds can be grouped as phytochemicals and its strong antioxidant effects serves as powerful reducing agents and aid in stabilization in synthesis of metallic nanoparticles [25,26]. Table 1 shows the phenolic compounds found within the coconut extract along with its chemical structure. The use of biologically sourced phytochemicals in nanoparticle synthesis is due to its biocompatibility especially in producing gold and silver nanoparticles for biomedical purposes [25,26].

Theoretically, micronutrient such as magnetic iron nanoparticles stimulate the production of biohydrogen through surface area and quantum size effect [6]. Therefore, the well-synthesized nanoparticles are extremely important for a fermentative hydrogen production system. In this study, magnetic iron nanoparticles was produced using hydrothermal method. The FESEM micrograph of magnetic iron nanoparticles showed that the average diameters were approximately 75 ± 6 nm in Fig. 1b). It is shown that some nanoparticles are spherical in shape while others are rod-like, still within the nano-size range. This polydisperse scattering are not as similar as previous studies that have monodisperse shapes [27,28]. The uneven dispersity of the shape may be due to non-optimised condition to the synthesis of the iron oxide nanoparticles such as the influence of iron precursors ratio, the type of base used and operational conditions like mixing temperature, agitation, and pH that can ensure better shape consistency [29]. For future study, the method would have to

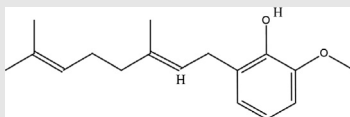
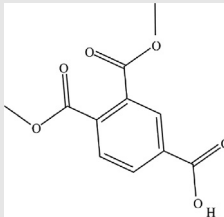
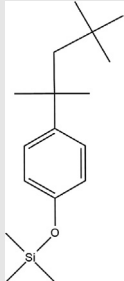
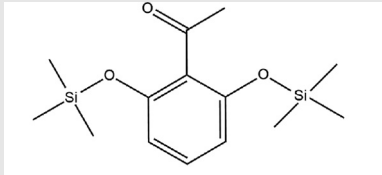
be tuned to ensure better monodisperse and more volume of the spherical iron nanoparticles rather than mixture of rods and spheres in one particle.

The crystalline phase and the nanoparticles were observed by using the X-ray diffraction powder (XRD) analysis. Fig. 1a) shows the X-ray power diffractograms of the iron oxide nanoparticles which are a series of peaks at $2\theta = 18.277^\circ$, 30.179° , 35.427° , 37.137° , 43.224° , 53.623° , 57.180° , 62.854° , 71.330° , and 74.384° and were assigned to (111), (220), (311), (222), (400), (422), (511), (440), (620), and (533) planes of cubic structures. The highest peak in the nanoparticle was at 2θ of 35.427° . The peaks present in Fig. 1a) shows matching to the crystallinity of magnetite Fe_3O_4 from standard PDF 00-065-073. These peaks are mostly similar to many research made previously on green synthesis of magnetite [30–32]. The size of the nanoparticles was calculated using the Scherer's equation ($D = K\lambda/\beta\cos\theta$) where K is the shape factor for a

typical value of 0.9, β is the full width at half maximum (FWHM) of a particular diffraction peak in radians, λ is the X-ray wavelength for iron at 1.54060 \AA , and θ is the Bragg angle [33]. The average size calculated using the equation from all the peaks from XRD result was at $89.67 \pm 13.06 \text{ nm}$.

The magnetic behaviour of the magnetite iron oxide nanoparticles was measured using a vibrating sample magnetometer (VSM). The magnetization moment measured was 44.025 emu/g which indicates that the product is ferromagnetic in nature because it has large and positive moment. The ferromagnetic nanoparticles turn into superparamagnetic due to its small nanoscale size. Thus, the magnetite formed from DES extracted coconut shell is superparamagnetic in nature [34]. This nature is in line with other studies made by previous researchers [27,31,35]. The average zeta potential of iron oxide nanoparticles was -7.305 mV . The negative charge zeta potential may be due to

Table 1 – The structure of phenolic compounds present in coconut extract.

Phenol	Chemical Structure
2-Nonaprenyl-6-methoxyphenol	
1,2,4-Benzenetricarboxylic acid, 1,2-dimethyl ester	
Trimethyl[4-(1,1,3,3-tetramethylbutyl)phenoxy]silane	
2',6'-Bis(trimethylsiloxy)acetophenone	

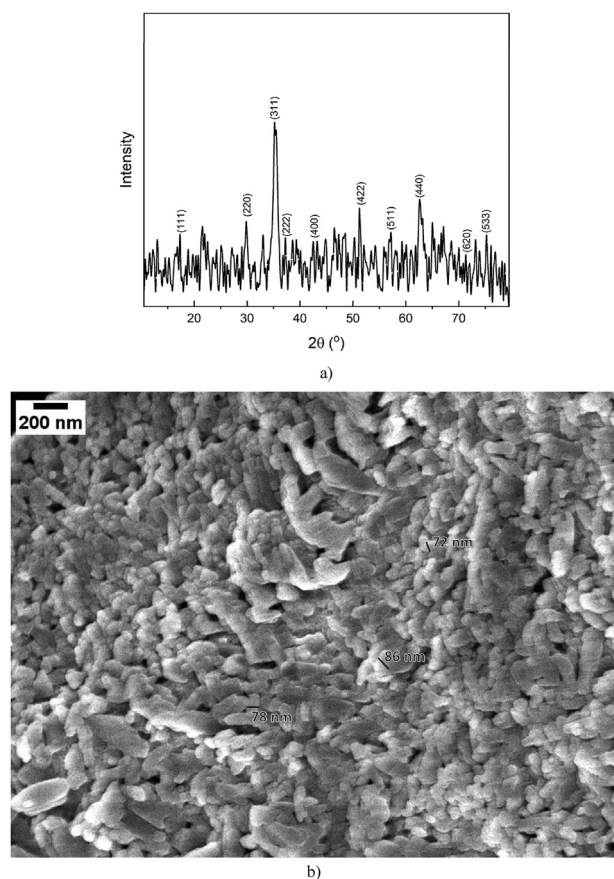


Fig. 1 – Characterization of green synthesized iron oxide nanoparticles using a) X-ray diffraction powder (XRD) analysis and b) field-emission scanning electron microscopy (FESEM).

the dissociation of Fe-OH and the formation of Fe-O that occurred between the iron salt precursor and the phenolic compounds from the coconut shell extraction [36,36]. Previous study on the synthesis of biocompatible iron oxide nanoparticles also had negative zeta potential result due to the presence of hydroxyl group from phenolic contents in plant extract [37,38]. The lower range than 15 mV shows that it is prone to coagulation and less stable, similar to previous study made by Solgado and colleagues where the green synthesized iron oxides have zeta potential range from -4.39 to -8.96 mV [38]. To overcome this in the future, changes to parameters such as pH levels during the experimental procedure may help to increase the zeta potential magnitude and in turn make the nanoparticles more stable [39].

Effects of magnetic iron nanoparticles concentration on biohydrogen production

The effect of supplementation of magnetic iron nanoparticles was conducted under batch process. The glucose consumption was estimated by dividing the amount of glucose consumed by the sum of the initial glucose. Biogas analysis showed that only hydrogen and carbon dioxide produced during the anaerobic fermentation which indicated that no

methanogens bacteria were present in the cultures used in this study. The results of the optimization experiment were tabulated in Table 2. It was found that 200 mg Fe/L of the supplementation of magnetic iron nanoparticles produced higher hydrogen production and yield compared to other concentration with 101.33 mL of hydrogen produced and yield of 0.7865 mol H₂/mol glucose. The trend showed that the increase of magnetic iron nanoparticles concentration may increase the volume of hydrogen produced as well as hydrogen yield. The addition of small amount of magnetite iron nanoparticles was able to increase the hydrogen yield by 72.33% than control. However, the pattern to concentration used is not proportionate. This may be due to the polydispersity of the iron oxide itself which may affect the surface reactivity area that is proven difficult to measure accurately using machinery or calculations due to its irregularity in shape [40]. Overall, the hydrogen yield from added nanoparticles are mostly higher than control however, it is not comparable to previous studies using magnetic iron nanoparticles for biohydrogen production due to different nanoparticles synthesis, size, substrates, seed and operational conditions used (Table 4). These different factors influence highly to the hydrogen yield. However, many studies using thermophilic conditions have proven to increase hydrogen yield [41–43]. Practically, increasing the fermentation temperature by applying thermophilic condition had been proven to enhance the hydrogen production as compared to mesophilic conditions, especially when the complex substrate was used in the system [5]. Higher temperature influence rapid metabolism activities of the bacteria and thus, indirectly improved the substrate utilization by the bacteria and hence, enhanced the hydrogen production [44].

The experiment was made in triplicates to get the average biogas produced for higher accuracy followed by calculation of hydrogen produced and applied to linear regression model for statistical analysis (Table 3). From the table, the low Rsquared indicates that the model does not fit the data very well. The regression model only explains about 36.42% of all the variability in the dataset. In regression, the R² coefficient is a statistical measure that represent how well the regression line approximates the real data points [5].

The hydrogen production rate and energy production rate also follow the same order to concentration as that of hydrogen produced and yield. This is due to the calculation for both relating to each other. Making 200 mg Fe/L having highest hydrogen production rate at 3.38 L H₂/L·d and energy production rate of 43.12 kJ H₂/L·d. This proves that the supplementation of 200 mg Fe/L of magnetic iron nanoparticles gives the highest impact not only on hydrogen gas production but also to the energy production rate. The limiting concentration of magnetic iron nanoparticles was at 300 mg Fe/L, where the biohydrogen produced, hydrogen yield, hydrogen production rate, and energy production rate decrease due to the inhibitory effect for the bacteria which was similar to previous study that found 303 mg Fe/L was inhibitory under Andrew's inhibition model since excess of iron content is reported to inhibit the bioactivity of hydrogen producing microorganisms [45].

From the results, sugar consumptions were higher for all samples in this study (>9.0 g/L) which indicates that the

Table 2 – The effects of magnetic iron nanoparticles on thermophilic mixed bacteria.

Concentration NP (mg Fe/L)	Cumulative Biogas (mL)	Vol H ₂ (mL)	mol H ₂	Glucose final (g/L)	Sugar utilization (g/L)	mol substrate consumed	Yield (mol H ₂ /mol sugar)	Cell concentration, X (g/L)	H ₂ Production Rate (L H ₂ /L·d)	Energy Production Rate (kJ H ₂ /L·d)	Final pH	HAc (mM)	HBu (mM)	HPr (mM)
0	104.50	58.80	0.0023	0.74	9.26	0.0051	0.4494	2.6750	1.96	25.03	4.25	34.26	61.03	77.78
25	64.20	44.13	0.0017	0.82	9.18	0.0051	0.3405	2.997	1.47	18.78	3.86	53.16	65.11	72.54
50	152.75	76.37	0.0030	0.84	9.16	0.0051	0.5906	3.067	2.55	32.50	3.70	56.40	69.00	58.10
100	200.00	93.57	0.0037	0.80	9.20	0.0051	0.7200	2.900	3.12	39.82	4.21	59.09	41.83	51.49
150	113.00	61.90	0.0024	0.80	9.20	0.0051	0.4763	2.903	2.06	26.34	4.16	56.51	33.46	87.43
200	221.29	101.33	0.0040	0.88	9.12	0.0051	0.7865	3.192	3.38	43.12	3.55	64.50	35.85	79.26
300	176.75	85.11	0.0033	0.90	9.10	0.0051	0.6624	3.280	2.84	36.22	4.10	63.35	72.55	50.63

*HAc: acetic acid; HBu: butyric acid; HPr: propionic acid.

operating condition of this experiment is highly suitable for the mixed culture to fully utilize the substrate. The control at 0 mg Fe/L has the lowest final substrate concentration which gives it the highest substrate consumption percentage followed by 100 mg Fe/L, 150 mg Fe/L, 25 mg Fe/L, 50 mg Fe/L, 200 mg Fe/L, and lastly 300 mg Fe/L. These results show that the lower concentration of magnetite has higher substrate uptake activity than those with higher concentrations. Previous studies mentioned that the low substrate consumption may be due to accumulation of liquid fermentation which becomes over acidification of cultures followed by the microbes only converting the limited fraction of the substrate at different concentrations due to rate limiting step in the process [45].

The highest cell concentration as shown in Table 2 is that of 300 mg Fe/L concentration followed by 200 mg Fe/L, 50 mg Fe/L, 25 mg Fe/L, 150 mg Fe/L, 100 mg Fe/L, and lastly 0 mg Fe/L. High cell concentration generally provide higher hydrogen production to the abundance of catalytically active sites to convert organic sources into hydrogen [46]. The cell concentration shows that the bacterial growth is rapid within the experimental procedure, but it does not portray direct correlation to the hydrogen production because of the rate limiting step of iron uptake by the bacteria.

The glucose degradation produces volatile fatty acids (VFAs) and soluble metabolite which can be connected to the low yields, which is proven in this study when there was no addition of iron oxide nanoparticles in control experiment, the amount of propionic acid produced was greater than acetic and butyric acid, and hence the hydrogen yield also decreased [47]. The results showed that addition of iron oxide nanoparticles increased the production of acetate and butyrate, whereas the production of propionate results in a small amount as compared to control. This scenario could be because the addition of NPs effectively directed the bacterial metabolism to produce more VFAs [10]. Moreover, since the experiments were conducted at optimal initial pH of 5.5, which is able to direct the metabolic pathway oriented toward the production of hydrogen allowing for higher yield [5].

The reduction of final pH compared to initial pH of 5.5 of the samples after 72-h cycle was due to the accumulation of volatile fatty acids produced in the mixed bacteria culture as the by-product of the fermentation process [48]. Among the different concentrations, the control with no added magnetic iron nanoparticles has the highest pH value at 4.25 whereas any addition of the nanoparticles will show reduction of pH level. This shows that the supplementation of magnetic iron nanoparticles lowers the final pH, showing a significant change in the environment within the mixed bacteria culture as compared to control. The pH value of 3.55 was the lowest for iron oxide concentration of 200 mg Fe/L. The acidic environment shows that possibly the acetate and butyrate metabolic pathways were utilized to generate the highest biohydrogen production among the other nanoparticles concentration [49,50].

The acetic acid production increases as the concentration of iron oxide nanoparticles increase. Thus, it can be said that the biohydrogen produced under this system was following the acetic pathway in which the presence of metal ion such as Fe³⁺ stimulates the hydrogenase enzyme reaction that

Table 3 – ANOVA for optimization with the presence of magnetic iron nanoparticles.

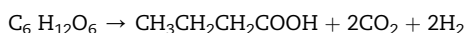
		Mean	Std. Deviation	N	Remark		
Descriptive Statistics	Hydrogen Production	74.46	20.52	7			
	NP Concentration	117.86	106.77	7			
Model Summary	R	R_{squared}	Adjusted R_{squared}	Std. Error of the Estimate			
	0.603	0.364	0.237	17.92	Not significant		
ANOVA	Model	Sum of Squares	Df	Mean Square	F	P value	
	Regression	920.23	1	920.23	2.864	0.151	
	Residual	1606.78	5	321.35			
	Total	2527.01	6				

significantly increase the electron transfer and this reaction increases the hydrogen production as well as cell growth [47,48]. As for butyric acid, the acid concentration in the sample also increases as the nanoparticles concentration increase but shows a sudden drop starting from 100 mg Fe/L and gradually goes upward until 300 mg Fe/L. In the higher nanoparticle concentrations, acetic acid production is more than butyric acid due to the stoichiometric chemical equation of converting glucose produces two parts of acetate with four parts of hydrogen whereas it produces only one part butyrate with two parts hydrogen as shown in the equation below [53]. Propionic acid shows gradual decrease from 0 mg Fe/L to 100 mg Fe/L followed by sharp jump at 150 mg Fe/L and gradually goes down again until 300 mg Fe/L. The highest propionic acid concentration at 150 mg Fe/L shows that the propionate metabolic pathway was favored under this concentration. The low biohydrogen production at this concentration is due to the propionic acid suppressing hydrogen-producing bacteria [54]. The propionate pathway produces two parts propionate while consuming two parts of hydrogen in the process [53]. Thus, fermentation with low production of propionic acid is more favored to avoid the consumption of hydrogen.

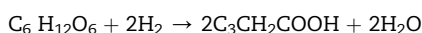
Acetate production:



Butyrate production:



Propionic production:



These results demonstrated that the mixed culture used in this system was able to adapt with the presence of magnetic iron nanoparticles up to a certain concentration. This can be seen from the difference in lag phase between control experiment and the one with the supplementation of magnetic iron nanoparticles, in which the lag phase was shorter by 7.12 h or at about 6.26 h as compared to 13.38 h in control (Table 6). This result was much better than previous studies probably due to difference in temperature condition, wherein thermophilic condition, the lag phase was shorter, between 3 and 9 h compare to about 18–24 h during mesophilic

fermentation [6,55]. It can be found that there were two factors that improved the hydrogen production yield in this study which firstly is due to thermophilic condition that stimulates the hydrogenase enzyme to act at its optimum capability [56,57]. Secondly, the addition of iron NPs that acts as a cofactor which accelerates the redox reaction during anaerobic fermentation of hydrogen [5,58].

Kinetics study of the effect of supplementation of magnetic iron nanoparticles

The kinetic study was done to investigate the effect of addition of iron nanoparticles on biohydrogen production by using different kinetics model. The best concentration from optimization experiment was used for this kinetic experiment, which was 200 mg Fe/L of iron oxide nanoparticles. Fig. 2 shows the pattern of the cumulative hydrogen produced with time that followed a typical growth curve consisting of lag, exponential and stationary phases for both control and added iron oxide nanoparticles samples during the experiment. The results show that the addition of iron oxide nanoparticles was able to produce more hydrogen compared to control experiment.

The addition of 200 mg Fe/L of iron oxide nanoparticles improved the volume of hydrogen produced, hydrogen yield, hydrogen production rate and the energy production rate as in Table 5. However, it was found that sugar consumption for control experiment was much better which may be due to the microbes having some limit in substrate conversion due to acidification from the accumulation of fermentation liquid [45]. The final pH shows that added magnetic iron nanoparticles is slightly acidic than that of control. This explains why the hydrogen production is higher due to accumulation of hydrogen producing acids such as acetic and butyric acid that are present in the mixture at the end of the experiment [48]. The production of butyric acid and acetic acid concentration was higher when iron oxide nanoparticle was present which reflects to higher amount of hydrogen produced. The system favors butyric acid production as compared to acetic acid since more butyric acid were produced in the sample compared to acetic acid. While it was found that the acetic acid formation in the sample with added iron oxide nanoparticle contains about 48.5% higher concentration than control experiment. The formation of high concentrations of acetic acid proved that the acetate pathway is highly responsible in the increase of hydrogen generation [62]. The

Table 4 – Studies on effect of magnetic iron nanoparticles in biohydrogen production.

Types	Synthesis	Size (nm)	Working Volume (mL)	Temperature (°C)	Optimum Concentration (mg Fe/L)	Substrate	Yield	References
Fe ₃ O ₄	Commercial	20	300	37	200	Glucose	260.9 mL H ₂ /g Glucose	[1]
Fe ₃ O ₄	Reduction-precipitation method	50	700	37	40	Glucose and Xylose	0.37 ± 0.004 mol H ₂ /mol sugar	[59]
Fe ₃ O ₄	Commercial	40–60	5500	35 ± 1	50	Glucose	12.97 mL H ₂ /g-VSS	[60]
Fe ₃ O ₄ (magnetic activated carbon)	Reflux process	Pore size 4.4	500	37	200	Glucose	214 mL H ₂ /g Glucose	[61]
Ni Fe ₂ O ₄ ferromagnetic	Coprecipitation method	Less than 50	500	37 and 55	200	Glucose	130 mL H ₂ /g Glucose	[11]
Fe ₃ O ₄	Green synthesis (hyacinth)	13.5 ± 3.7	350	37	20	Rice straw hydrolysate	83.20 ± 2.19 mL H ₂ /g substrate	[31]
Fe ₃ O ₄	Green synthesis (green coconut shell)	75 ±6	100	55	200	Glucose	11.11 ml H ₂ /g sugar; 0.79 mol H ₂ /mol sugar	This study

Table 5 – The effects of adding magnetic nanoparticles compared to control.

Concentration NP (mg Fe/L)	Cumulative Biogas (mL)	Vol H ₂ (mL)	mol H ₂	Glucose final (g/L)	Sugar utilization (g/L)	mol substrate consume	Yield (mol H ₂ /mol sugar)	Cell concentration, X (g/L)	H ₂ Production Rate (L H ₂ /L·d)	Energy Production Rate (kJ H ₂ /L·d)	Final pH	Final HAc (mM)	Final HBU (mM)	Final HPr (mM)
0	322	137.9	0.0054	0.57	9.43	0.0131	0.4145	2.07	1.84	23.50	4.37	36.89	59.52	94.22
200	375	157.3	0.0062	0.87	9.13	0.0127	0.4880	3.16	2.10	26.78	4.28	60.53	66.63	50.62

Table 6 – Dynamically fitted parameters according to Gompertz and Monod Model.

Concentration (mg Fe/L)	P _{max} (mL)	R _m (mL/h)	λ (hour)	R _{squared} Gompertz	μ _{max} (h ⁻¹)	K _s (g/L)	R _{squared} Monod
0	44.60	1.65	13.38	0.972	0.0065	10.44	0.889
200	50.69	3.30	6.26	0.998	0.0060	10.09	0.994

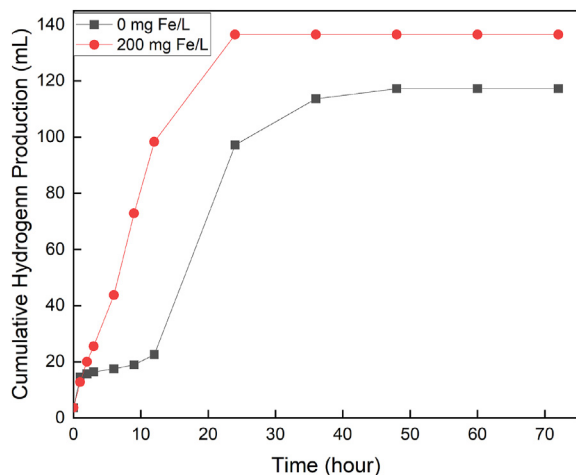
acetic acid production of 200 mg Fe/L increases to almost two folds of control while the formation of propionic acid was more significant in control experiment with nearly 60.2% higher than the sample with iron oxide nanoparticles. This hydrogen consuming acid shows the reason why the formation of hydrogen is lower in control experiment [63].

The results from this experiment were then applied onto the Monod and Gompertz model using MATLAB software to determine the dynamically fitted parameters according to the models. Gompertz model was selected for kinetic analysis as it is the best fit to represent the exponential relationship between specific growth rate and lag phase duration which is not explained in other models [64]. Prediction of lag phase during the fermentation process is important as it is related to the fermentation productivity. By cutting down the lag phase and maintaining the system in exponential phase, this might help in increasing production during the fermentation [6]. Furthermore, fermentation product was produced rapidly during exponential phase thus, kinetic analysis needs to be done during this stage in order to fully describe the relationship between the cell growth and production rate. Gompertz model is much suitable in describing kinetic study for biogas fermentation as it is related to metabolic reaction of bacteria that resulted in producing the gas. Moreover, metabolic reaction inside bacteria is related to the energy conservation. The biogas production is a product of energy conservation that is also important in cells growth, hence it leads to an accurate representation of the lag phase [65]. Therefore, the kinetic analysis using Gompertz to determine the maximum hydrogen production potential (P_{max}), maximum hydrogen production rate (R_m) and lag phase for all batches were

calculated and tabulated in Table 6. Based on the Gompertz model, the maximum hydrogen production, P_{max} of the added magnetite was 12.78% higher than control at 50.69 mL. The maximum hydrogen production rate, R_m of 200 mg Fe/L was 3.30 mL/h whereas control was at 1.65 mL/h, showing a 66.67% increase. Lastly, the lag phase, λ of added iron is 7.12 h shorter than control at 6.26 h. The coefficient of determination, R² values for Gompertz model were about 0.97 for all regression, showed that a strong correlation between the experimental data and the fitted curve. The addition of iron oxide nanoparticles caused the dramatic decrease in lag phase time from approximately 13 h in control experiment to less than 6 h. Moreover, the shorter lag phase had influenced the increase in maximum hydrogen production rate, R_m compared to the control sample. Thus, these results have suggested that the NPs have a significant influence on the kinetic of hydrogen production than the total biogas production due to glucose utilization [45].

Monod model is used in this research to study the effect of the substrate used in the fermentation medium to the mixed bacteria culture. Small changes may affect the bacteria entirely for it to adapt to new changes. Naturally, when new nutrients are introduced to the bacterial cell, the cell will adapt itself to the new environment by producing the required enzyme. This also means that all nutrients can limit the rate of fermentation when presence of concentrations that are too high or too low. As the concentration of the nutrient increases, the bacterial growth rate will increase until the maximum value and the growth will maintain until the nutrient reaches an inhibitory level, which then causes the growth rate to fall. Thus, from Monod equation, the effect of supplementation of magnetic iron nanoparticles can be observed from the saturation constant, K_s. The value of saturation constant, K_s showed the concentrations that support a half-maximal rate of the bacterial growth under respective condition [66]. From the linearized Monod model, the values of K_s and μ_{max} are in negative integers due to negative intercept in linearized Monod model which suggested that these bacteria need more energy to maintain the cells [67].

The K_s value decreased with addition of magnetite in the fermentation culture, at magnitude of 10.09 g/L glucose. This K_s value indicates that this fermentation process utilizes the sugar metabolism which was in line with the high value of sugar utilization shown in this study. The maximum growth rate, μ_{max} is achieved when the substrate concentration, S is higher than K_s and the concentration of other essential nutrients are the same. The saturation constant K_s is the approximate division between the lower concentration range where μ is essentially linearly related to substrate and the higher rate where μ becomes independent of any concentration of the nutrient supplied. However, the range of nutrient/substrate concentration used in this study may have

**Fig. 2 – The cumulative biohydrogen production of 200 mg Fe/L magnetite compared to control.**

influenced whether enhancing or inhibiting of fermentation activity, thus, results may vary with each microorganism, chemical species, and growth conditions [68].

Conclusion

Enhancing the biohydrogen production using thermophilic mixed bacteria is feasible with the presence of magnetic iron nanoparticles during the fermentation process. The supplementation of nanoparticles onto the fermentation process was able to increase the hydrogen production yield by 72.33% and also produced higher energy production rate (EPR) of 43.12 kJ H₂/L·d under the presence of the optimum amount of magnetic iron nanoparticle (200 mg Fe/L). This result proved that the supplementation of magnetic iron nanoparticles that act as micronutrient during the fermentation process was able to stimulate the hydrogenase enzyme to release more hydrogen. The kinetics parameters of Gompertz and Monod model are also dominated by addition of 200 mg Fe/L magnetic iron nanoparticles compared to control. Maximum hydrogen production, P_{max} of added magnetic iron nanoparticle was 50.69 mL, hydrogen production rate, R_m was 3.30 mL/h and lag phase, λ was 6.26 h. This is followed by Monod kinetics of specific growth rate, μ_{max} of 0.006 h⁻¹ and cell growth saturation coefficient, K_s of 10.09 g/L.

Declaration of competing interest

The authors declare that they have no known competing financial interests or personal relationships that could have appeared to influence the work reported in this paper.

Acknowledgement

The author would like to thank the Ministry of Higher Education Malaysia for granted the fund for this research under the Fundamental Research Grant Scheme, FRGS/1/2019/TK07/UIAM/02/1 (FRGS19-105-0714) and to International Islamic University specifically to Department of Chemical Engineering & Sustainability, Kulliyah of Engineering for research facilities and support.

REFERENCES

- [1] Cheng J, et al. Improving hydrogen and methane co-generation in cascading dark fermentation and anaerobic digestion: the effect of magnetite nanoparticles on microbial electron transfer and syntrophism. *Chem Eng J* November 2019;397:125394. <https://doi.org/10.1016/j.cej.2020.125394>.
- [2] Soares JF, Confortin TC, Todero I, Mayer FD, Mazutti MA. Dark fermentative biohydrogen production from lignocellulosic biomass: technological challenges and future prospects. *Renew Sustain Energy Rev* October 2019;117:2020. <https://doi.org/10.1016/j.rser.2019.109484>.
- [3] Ramírez-Morales JE, Tapia-Venegas E, Toledo-Alarcón J, Ruiz-Filippi G. Simultaneous production and separation of biohydrogen in mixed culture systems by continuous dark fermentation. *Water Sci Technol* 2015;71(9):1271–85. <https://doi.org/10.2166/wst.2015.104>.
- [4] Mishra P, Krishnan S, Rana S, Singh L, Sakinah M, Ab Z. Outlook of fermentative hydrogen production techniques : an overview of dark , photo and integrated dark-photo fermentative approach to biomass. *Energy Strategy Rev* 2019;24:27–37. <https://doi.org/10.1016/j.esr.2019.01.001>.
- [5] Engliman NS, Abdul PM, Wu S. Influence of iron (II) oxide nanoparticle on biohydrogen production in thermophilic mixed fermentation. *Int. J. of hydrogen energy xxx* 2017;1e12:1–12. no. li.
- [6] Han H, Cui M, Wei L, Yang H, Shen J. Enhancement effect of hematite nanoparticles on fermentative hydrogen production. *Bioresour Technol* 2011;102(17):7903–9. <https://doi.org/10.1016/j.biortech.2011.05.089>.
- [7] Mullai P, Yogeswari MK, Sridevi K. Bioresource Technology Optimisation and enhancement of biohydrogen production using nickel nanoparticles – a novel approach, 141; 2013. p. 212–9.
- [8] Mohanraj S, Anbalagan K, Rajaguru P. Effects of phyto-genic copper nanoparticles on fermentative hydrogen production by *Enterobacter cloacae* and *Clostridium acetobutylicum*. *Int J Hydrogen Energy* 2016;41(25):10639–45. <https://doi.org/10.1016/j.ijhydene.2016.04.197>.
- [9] Lin CY, Lay CH. A nutrient formulation for fermentative hydrogen production using anaerobic sewage sludge microflora. *Int J Hydrogen Energy* 2005;30(3):285–92. <https://doi.org/10.1016/j.ijhydene.2004.03.002>.
- [10] Lin R, et al. Enhanced dark hydrogen fermentation by addition of ferric oxide nanoparticles using *Enterobacter aerogenes*. *Bioresour Technol* 2016;207:213–9. <https://doi.org/10.1016/j.biortech.2016.02.009>.
- [11] Zhang J, Zhao W, Yang J, Li Z, Zhang J, Zang L. Comparison of mesophilic and thermophilic dark fermentation with nickel ferrite nanoparticles supplementation for biohydrogen production. *Bioresour Technol* 2021;329(3501):124853. <https://doi.org/10.1016/j.biortech.2021.124853>.
- [12] Abdullah MF, Md Jahim J, Abdul PM, Mahmud SS. Effect of carbon/nitrogen ratio and ferric ion on the production of biohydrogen from palm oil mill effluent (POME). *Biocatal Agric Biotechnol* 2020;23:101445. <https://doi.org/10.1016/j.cbac.2019.101445>.
- [13] Reddy K, et al. Biohydrogen production from sugarcane bagasse hydrolysate: effects of pH, S/X, Fe²⁺, and magnetite nanoparticles. *Environ Sci Pollut Res* 2017;24(9):8790–804. <https://doi.org/10.1007/s11356-017-8560-1>.
- [14] Nasr M, Tawfik A, Ookawara S, Suzuki M, Kumari S, Bux F. Continuous biohydrogen production from starch wastewater via sequential dark-photo fermentation with emphasize on maghemite nanoparticles. *J Ind Eng Chem* 2015;21:500–6. <https://doi.org/10.1016/j.jiec.2014.03.011>.
- [15] Baek G, Jung H, Kim J, Lee C. A long-term study on the effect of magnetite supplementation in continuous anaerobic digestion of dairy effluent – magnetic separation and recycling of magnetite. *Bioresour Technol* 2017;241:830–40. <https://doi.org/10.1016/j.biortech.2017.06.018>.
- [16] Teja AS, Koh PY. Synthesis, properties, and applications of magnetic iron oxide nanoparticles. *Prog Cryst Growth Char Mater* 2009;55(1–2):22–45. <https://doi.org/10.1016/j.pcrysgrow.2008.08.003>.
- [17] Smith EL, Abbott AP, Ryder KS. Deep Eutectic Solvents (DESs) and Their Applications 2014. <https://doi.org/10.1021/cr300162p>.

- [18] Cunha SC, Fernandes JO. Extraction techniques with deep eutectic solvents. *TrAC, Trends Anal Chem* 2018;105:225–39. <https://doi.org/10.1016/j.trac.2018.05.001>.
- [19] Aziz AHA, Engliman NS, Mansor MF, Nasaruddin RR. Extraction of phenolic compound using natural deep eutectic solvent from biomass waste. *IOP Conf Ser Mater Sci Eng* 2021;1192(1):012001. <https://doi.org/10.1088/1757-899x/1192/1/012001>.
- [20] Maheswari KC, Reddy. Green synthesis of magnetite nanoparticles through leaf extract of *Azadirachta indica*. *Jacs Dir* 2016;2(4):189–91.
- [21] Sivagurunathan P, Sen B, Lin CY. High-rate fermentative hydrogen production from beverage wastewater. *Appl Energy* 2015;147:1–9. <https://doi.org/10.1016/j.apenergy.2015.01.136>.
- [22] Jamali NS, Md Jahim J, O-Thong S, Jehlee A. Hydrodynamic characteristics and model of fluidized bed reactor with immobilised cells on activated carbon for biohydrogen production. *Int J Hydrogen Energy* 2019;44(18):9256–71. <https://doi.org/10.1016/j.ijhydene.2019.02.116>.
- [23] Kumar G, Sen B, Sivagurunathan P, Lin CY. High rate hydrogen fermentation of cello-lignin fraction in de-oiled jatropha waste using hybrid immobilized cell system. *Fuel* 2016;182:131–40. <https://doi.org/10.1016/j.fuel.2016.05.088>.
- [24] Kolniak-Ostek J, Oszmianński J, Wojdyto A. Effect of l-ascorbic acid addition on quality, polyphenolic compounds and antioxidant capacity of cloudy apple juices. *Eur Food Res Tech* 2013;236(5):777–98. <https://doi.org/10.1007/s00217-013-1931-z>.
- [25] Park Y, Hong YN, Weyers A, Kim YS, Linhardt RJ. Polysaccharides and phytochemicals: a natural reservoir for the green synthesis of gold and silver nanoparticles. *IET Nanobiotechnol* 2011;5(3):69–78. <https://doi.org/10.1049/iet-nbt.2010.0033>.
- [26] Lee J, et al. Green synthesis of phytochemical-stabilized Au nanoparticles under ambient conditions and their biocompatibility and antioxidative activity. *J Mater Chem* 2011;21(35):13316–26. <https://doi.org/10.1039/c1jm11592h>.
- [27] Mahdavi M, Namvar F, Bin Ahmad M, Mohamad R. Green biosynthesis and characterization of magnetic iron oxide (Fe₃O₄) nanoparticles using seaweed (*Sargassum muticum*) aqueous extract. *Molecules* 2013;18(5):5954–64. <https://doi.org/10.3390/molecules18055954>.
- [28] Azizi A. Green synthesis of Fe₃O₄ nanoparticles and its application in preparation of Fe₃O₄/cellulose magnetic nanocomposite: a suitable proposal for drug delivery systems. *J Inorg Organomet Polym Mater* 2020;30(9):3552–61. <https://doi.org/10.1007/s10904-020-01500-1>.
- [29] Zia M, Phull AR, Ali JS. Challenges of iron oxide nanoparticles. *Powder Technol* 2016;7(6):49–67.
- [30] Venkateswarlu S, Natesh Kumar B, Prathima B, Anitha K, Jyothi NVV. A novel green synthesis of Fe₃O₄-Ag core shell recyclable nanoparticles using *Vitis vinifera* stem extract and its enhanced antibacterial performance. *Phys B Condens Matter* 2015;457:30–5. <https://doi.org/10.1016/j.physb.2014.09.007>.
- [31] Zhang Q, Zhang Y, Li Y, Ding P, Xu S, Cao J. Green synthesis of magnetite nanoparticle and its regulatory effect on fermentative hydrogen production from lignocellulosic hydrolysate by *Klebsiella* sp. *Int J Hydrogen Energy* 2021;46(39):20413–24. <https://doi.org/10.1016/j.ijhydene.2021.03.142>.
- [32] Das C, et al. Green synthesis, characterization and application of natural product coated magnetite nanoparticles for wastewater treatment. *Nanomaterials* 2020;10(8):1–19. <https://doi.org/10.3390/nano10081615>.
- [33] Jamzad M, Kamari Bidkorpheh M. Green synthesis of iron oxide nanoparticles by the aqueous extract of *Laurus nobilis* L. leaves and evaluation of the antimicrobial activity. *J Nanostructure Chem.* 2020;10(3):193–201. <https://doi.org/10.1007/s40097-020-00341-1>.
- [34] Ningthoujam RS. Synthesis and characterization of borides, carbides, and nitrides and their applications. Elsevier Inc.; 2017.
- [35] Chen L, Long Y, Leng Z, Hu J, Yu X, Yu X. Facile synthesis and special phase transformation of hydrophilic iron oxides nanoparticles. *J Nanomater* 2017;2017. <https://doi.org/10.1155/2017/1064863>.
- [36] Reddy PM, Chang KC, Liu ZJ, Chen CT, Ho YP. Functionalized magnetic iron oxide (Fe₃O₄) nanoparticles for capturing gram-positive and gram-negative bacteria. *J Biomed Nanotechnol* 2014;10(8):1429–39. <https://doi.org/10.1166/jbn.2014.1848>.
- [37] Demirbas A, Kislakci E, Karaagac Z, Onal I, Ildiz N, Ocsoy I. Preparation of biocompatible and stable iron oxide nanoparticles using anthocyanin integrated hydrothermal method and their antimicrobial and antioxidant properties. *Mater Res Express* 2019;6(12). <https://doi.org/10.1088/2053-1591/ab540c>. 0–7.
- [38] Salgado P, Márquez K, Rubilar O, Contreras D, Vidal G. The effect of phenolic compounds on the green synthesis of iron nanoparticles (Fe_xO_y-NPs) with photocatalytic activity. *Appl Nanosci* 2019;9(3):371–85. <https://doi.org/10.1007/s13204-018-0931-5>.
- [39] Holmes M, et al. Zeta potential measurement for water treatment coagulation control. *Aust. Aust. Water Assoc.*, no. May 2015:1–8 [Online]. Available: <https://www.researchgate.net/publication/280575005>.
- [40] Bau S, Witschger O, Gensdarmes F, Thomas D. Evaluating three direct-Reading instruments based on diffusion charging to measure surface area concentrations in polydisperse nanoaerosols in molecular and transition regimes. *J Nanoparticle Res* 2012;14(11). <https://doi.org/10.1007/s11051-012-1217-6>.
- [41] Liu Z, et al. States and challenges for high-value biohythane production from waste biomass by dark fermentation technology. *Bioresour Technol* 2013;135:292–303. <https://doi.org/10.1016/j.biortech.2012.10.027>.
- [42] Lay CH, et al. Recent trends and prospects in biohythane research: an overview. *Int J Hydrogen Energy* 2020;45(10):5864–73. <https://doi.org/10.1016/j.ijhydene.2019.07.209>.
- [43] Wang J, Wan W. Effect of temperature on fermentative hydrogen production by mixed cultures. *Int J Hydrogen Energy* 2008;33(20):5392–7. <https://doi.org/10.1016/j.ijhydene.2008.07.010>.
- [44] Zainal BS, Ahmad MA, Danaee M, Jamadon N, Mohd NS, Ibrahim S. Integrated system technology of pome treatment for biohydrogen and biomethane production in Malaysia. *Appl Sci* 2020;10(3):1–18. <https://doi.org/10.3390/app10030951>.
- [45] Malik SN, Pugalenth V, Vaidya AN, Ghosh PC, Mudliar SN. Kinetics of nano-catalysed dark fermentative hydrogen production from distillery wastewater. *Energy Proc* 2014;54:417–30. <https://doi.org/10.1016/j.egypro.2014.07.284>.
- [46] Lee DY, Li YY, Oh YK, Kim MS, Noike T. Effect of iron concentration on continuous H₂ production using membrane bioreactor. *Int J Hydrogen Energy* 2009;34(3):1244–52. <https://doi.org/10.1016/j.ijhydene.2008.11.093>.
- [47] Infantes D, González Del Campo A, Villaseñor J, Fernández FJ. Influence of pH, temperature and volatile fatty acids on hydrogen production by acidogenic fermentation. *Int J Hydrogen Energy* 2011;36(24):15595–601. <https://doi.org/10.1016/j.ijhydene.2011.09.061>.
- [48] Taifor AF, Zakaria MR, Mohd Yusoff MZ, Toshinari M, Hassan MA, Shirai Y. Elucidating substrate utilization in biohydrogen production from palm oil mill effluent by

- Escherichia coli. *Int J Hydrogen Energy* 2017;42(9):5812–9. <https://doi.org/10.1016/j.ijhydene.2016.11.188>.
- [49] Hwang Y, Sivagurunathan P, Lee MK, Yun YM, Song YC, Kim DH. Enhanced hydrogen fermentation by zero valent iron addition. *Int J Hydrogen Energy* 2019;3387–94. <https://doi.org/10.1016/j.ijhydene.2018.06.015>.
- [50] Malik SN, Rena, Kumar S. Enhancement effect of zero-valent iron nanoparticle and iron oxide nanoparticles on dark fermentative hydrogen production from molasses-based distillery wastewater. *Int J Hydrogen Energy* 2021;46(58):29812–21. <https://doi.org/10.1016/j.ijhydene.2021.06.125>.
- [53] Wattiaux MA, Uddin ME, Letelier P, Jackson RD, Larson RA. Emission and mitigation of greenhouse gases from dairy farms : the cow , the manure , and the field. *Appl. Anim. Sci.* 2019;35(2):238–54. <https://doi.org/10.15232/aas.2018-01803>.
- [54] Wang J, Wan W. Effect of Fe²⁺ concentration on fermentative hydrogen production by mixed cultures. *Int J Hydrogen Energy* 2008;33(4):1215–20. <https://doi.org/10.1016/j.ijhydene.2007.12.044>.
- [55] Taherdanak M, Zilouei H, Karimi K. Investigating the effects of iron and nickel nanoparticles on dark hydrogen fermentation from starch using central composite design. *Int J Hydrogen Energy* 2015;40(38):12956–63. <https://doi.org/10.1016/j.ijhydene.2015.08.004>.
- [56] Bielen AAM, Verhaart MRA, Van Der Oost J, Kengen SWM. Biohydrogen production by the thermophilic bacterium *Caldicellulosiruptor saccharolyticus*: current status and perspectives. 2013. p. 52–85. <https://doi.org/10.3390/life3010052>.
- [57] Sun H, et al. Manganese ferrite nanoparticles enhanced biohydrogen production from mesophilic and thermophilic dark fermentation. *Energy Rep* 2021;7:6234–45. <https://doi.org/10.1016/j.egy.2021.09.070>.
- [58] Frey M. Hydrogenases: hydrogen-activating enzymes. *Chembiochem* 2002;3(2–3):153–60. [https://doi.org/10.1002/1439-7633\(20020301\)3:2/3<153::AID-CBIC153>3.0.CO;2-B](https://doi.org/10.1002/1439-7633(20020301)3:2/3<153::AID-CBIC153>3.0.CO;2-B).
- [59] Zhang Q, Li Y, Jiang H, Liu Z, Jia Q. Enhanced biohydrogen production influenced by magnetic nanoparticles supplementation using *Enterobacter cloacae*. *Waste and Biomass Valorization* 2021;12(6):2905–13. <https://doi.org/10.1007/s12649-020-01002-8>.
- [60] Zhong D, Li J, Ma W, Xin H. Magnetite nanoparticles enhanced glucose anaerobic fermentation for bio-hydrogen production using an expanded granular sludge bed (EGSB) reactor. *Int J Hydrogen Energy* 2020;45(18):10664–72. <https://doi.org/10.1016/j.ijhydene.2020.01.095>.
- [61] Fan C, Zhang J, Zang L. Improving biohydrogen evolution from glucose with magnetic activated carbon. *Water Air Soil Pollut* 2019;230(5). <https://doi.org/10.1007/s11270-019-4155-4>.
- [62] Choi J, Ahn Y. Biohydrogen fermentation from sucrose and piggery waste with high levels of bicarbonate alkalinity. *Energies* 2015;8:1716–29. <https://doi.org/10.3390/en8031716>.
- [63] Patel SKS, Lee JK, Kalia VC. Nanoparticles in biological hydrogen production: an overview. *Indian J Microbiol* 2018;58(1):8–18. <https://doi.org/10.1007/s12088-017-0678-9>.
- [64] Okpokwasili GC, Nweke CO. *Microbial growth and substrate utilization kinetics* 2005;5(4):305–17.
- [65] Wang J, Wan W. Experimental design methods for fermentative hydrogen production: a review. *Int J Hydrogen Energy* 2009;34(1):235–44. <https://doi.org/10.1016/j.ijhydene.2008.10.008>.
- [66] Nath K, Muthukumar M, Kumar A, Das D. Kinetics of two-stage fermentation process for the production of hydrogen. *Int J Hydrogen Energy* 2008;33(4):1195–203. <https://doi.org/10.1016/j.ijhydene.2007.12.011>.
- [67] Russell JB, Cook GM. *Energetics of bacterial growth : balance of anabolic and catabolic reactions*. *Microbiol Rev* 1995;59(1):48–62.
- [68] Gadhe A, Sonawane SS, Varma MN. Kinetic analysis of biohydrogen production from complex dairy wastewater under optimized condition. *Int J Hydrogen Energy* 2014;39(3):1306–14. <https://doi.org/10.1016/j.ijhydene.2013.11.022>.